Exploring The Role Of Piezo1 Mechanosensor In Human Monocyte Derived Dendritic Cell Migration

A Thesis

submitted to

Indian Institute of Science Education and Research Pune in partial fulfilment of the requirements for the BS-MS Dual Degree Programme

by

Desai Milie Mitesh

Indian Institute of Science Education and Research Pune

Dr. Homi Bhabha Road,

Pashan, Pune 411008, INDIA.

Date: April, 2023

Under the guidance of

Supervisor: Dr. Dipyaman Ganguly,

CSIR-Indian Institute of Chemical Biology

From May 2022 to Mar 2023

INDIAN INSTITUTE OF SCIENCE EDUCATION AND RESEARCH PUNE

Certificate

This is to certify that this dissertation entitled **Exploring The Role Of Piezo1 Mechanosensor In Human Monocyte Derived Dendritic Cell Migration** towards the partial fulfilment of the BS-MS dual degree programme at the Indian Institute of Science Education and Research, Pune represents study/work carried out by **Desai Milie Mitesh** at Indian Institute of Science Education and Research under the supervision of Dr. Dipyaman Ganguly, CSIR Indian Institute of Chemical Biology, during the academic year 2022-2023.

Sincerely,

Dipyaman Ganguly

Kolkata, India

Date: 12.4.2023

Committee:

Dr. Dipyaman Ganguly

Dr. Satyajit Rath

To my parents. Thanks for always motivating me to take my own path in life.

Declaration

I hereby declare that the matter embodied in the report entitled **Exploring The Role Of Piezo1 Mechanosensor In Human Monocyte Derived Dendritic Cell Migration** are the results of the work carried out by me at the Department of Biology, Indian Institute of Science Education and Research, Pune, under the supervision of Dr. Dipyaman Ganguly and the same has not been submitted elsewhere for any other degree.

Desai Milie Mitesh

Date: 10th April 2023

Table of Contents

List of Figures

Abstract

Dendritic cells (DC) act as the sentinels of the immune system, which survey the blood and tissue for any foreign antigen and, upon antigen recognition, activate and modulate the behaviour of the adaptive immune system. Due to their function, migration becomes a crucial aspect of DC biology and is dependent on biochemical signals and specific adhesion molecules. Mechanical stimuli influence DC migration; however, the molecular mechanism behind mechanosensation in DC migration is not well understood. Piezo1, a recently discovered mechanosensitive calcium ion channel, needs only mechanical stimuli for its activation. It is shown to be well expressed in mammals, including the cells of the human immune system, making Piezo1 an excellent candidate for the mechanosensory ion channel in DC migration. We used GsMTx4, a peptide inhibitor of Piezo1, to explore its role in the migration of human monocyte-derived dendritic cells (MoDCs), which are in-vitro generated DC. We report that Piezo1 inhibition does not affect the motility of mature and immature MoDCs. Furthermore, Piezo1 expression gets downregulated upon MoDC maturation. However, Piezo1 inhibition reduces the 3D chemokine-induced directional migration of immature MoDCs. Our study suggests that Piezo1 directly influences the directed migration in immature MoDC, but MoDCs migrate in a Piezo1-independent manner upon maturation.

Acknowledgements

I would like to take this opportunity to express my heartfelt gratitude to all those who have supported and encouraged me throughout my journey in completing my master's degree.

First and foremost, I would like to extend my sincere thanks to my supervisor Dr. Dipyaman Ganguly, for making this study possible. Their invaluable guidance, support, and patience throughout my research have been crucial in shaping my work and helping me stay motivated.

I would also like to acknowledge the members of my lab who created a beautiful environment to work in which contributed to my research project in various ways. A big thanks to my mentor Dr. Chinky Shiu Chen Liu for guiding me at throughout my project. Thank you to all the seniors, Purbita Bandhopadhyay, Jafar Sarif, Ranit D' Rozario, Bishnu P Sinha, Md Asmaul Haque for their support, advice, and technical expertise have been incredibly helpful in shaping my research and helping me overcome challenges. I am also grateful to my labmates and friends Shrestha Pathnayak, Shreya Roy, Suravi mukherjee and Rituparna Jana for their help and support throughout.

I am also grateful to my lunch-friends for their constant encouragement, and for always being there to listen and provide support when I needed it the most. Their unwavering support has kept me going during times of stress and self-doubt.

Last but not least, I would like to thank my family for their unwavering love and support. Their encouragement and belief in me have been the driving force behind my success, and I am forever grateful for their guidance and sacrifices.

Once again, I thank all those who have contributed to my success, and I am honored to have had the opportunity to work with such wonderful people.

Contributions

Contributor name	Contributor role
Dr. Dipyaman Ganguly, Desai Milie Mitesh, Dr. Chinky Shiu Chen Liu	Conceptualization Ideas
Dr. Dipyaman Ganguly, Desai Milie Mitesh, Dr. Chinky Shiu Chen Liu	Methodology
-	Software
Desai Milie Mitesh, Dr. Chinky Shiu Chen Liu	Validation
Desai Milie Mitesh	Formal analysis
Desai Milie Mitesh	Investigation
-	Resources
Desai Milie Mitesh	Data Curation
Desai Milie Mitesh	Writing - original draft preparation
Dr. Dipyaman Ganguly, Desai Milie Mitesh	Writing - review and editing
-	Visualization
Dr. Dipyaman Ganguly	Supervision
Dr. Dipyaman Ganguly, Dr. Chinky Shiu Chen Liu	Project administration
Dr. Dipyaman Ganguly	Funding acquisition

This contributor syntax is based on the Journal of Cell Science CRediT Taxonomy[1].

[1] https://journals.biologists.com/jcs/pages/author-contributions

Chapter 1 Introduction

The immune system is said to have evolved to defend the body from foreign invaders. The immune system has two primary components: the innate immune system and the adaptive immune system. The innate immune system is the first line of defence responsible for phagocytising any foreign antigen and generating an inflammatory response to invading pathogens (Turvey and Broide, 2010). The adaptive immune response is responsible for a target specific response generated in case of a prolonged infection or inflammation (Bonilla and Oettgen, 2010). Dendritic cells are a link between the innate and adaptive immune systems. They act as sentinel cells, surveying tissues for any antigen and upon antigen recognition, they express part of the antigen on their cell surface. In the lymph nodes, the T cells recognise this antigen via specialised surface proteins called the T cell receptor complex (Théry and Amigorena, 2001). Depending on the cellular state of the antigen-presenting dendritic cell, they alter the response of the T cells and, subsequently, the immune system. If DCs receive pro-inflammatory signals during antigen recognition, they turn into a mature state and prime the T cells' function against the inflammation-causing agent (Banchereau and Steinman, 1998). However, a lack of pro-inflammatory signals causes the DCs to induce a state of tolerance in T cells resulting in a dampening of response towards that response (Iberg *et al.*, 2017). Thus DC are potent regulators of the immune system. The function and migration of DC are closely linked. The role of migration for DC function in the skin, lungs, intestine and central nervous system is well explored and reviewed (Worbs *et al.*, 2017). DC migration also influences the pathogenesis of inflammatory diseases like atherosclerosis, rheumatoid arthritis and psoriasis (Worbs *et al.*, 2017).

DC function and migration are well regulated by biochemical cues from pathogens and damaged tissue. Recognition of conserved molecules structures associated with pathogens (e.g., lipopolysaccharide found on bacterial cells wall) and damaged tissue (e.g. intracellular nucleic acid released by dying cells) via specialised receptors called pattern recognition receptor (PRR) lead to the maturation of DCs (Al-Ashmawy, 2018). Upon maturation, DCs upregulate surface markers like CD80, CD83, CD40 and MHC-II (Jin *et al.*, 2010). Mature DCs are shown to be more effective in antigen presentation than immature DCs (Théry and Amigorena, 2001), suggesting the biochemical cues also eventually affect antigen presentation. Chemokines are small chemical molecules that signal for migration of the immune cells, called chemotaxis. A prominent regulator of chemotaxis in DC is the CC

chemokine receptor 7 (CCR7), a g protein coupled receptor, that binds to chemokines CC chemokine ligand 19 and 21 (CCL19 and CCl21) (Förster *et al.*, 2008). Signal transduction along the CCR7-CCL19/CCL21 axis is a critical regulator of migration in dendritic cells during both steady state and inflammation (Ohl *et al.*, 2004). Upon maturation, DCs are also shown to upregulate the expression of CCR7. Kinases like RhoGTPases that regulate the activity and distribution of cytoskeletal elements, along with adhesion molecules like integrins, also contribute to the regulation of DC migration as reviewed (Vicente-Manzanares and Sánchez-Madrid, 2004).

DCs receive a variety of mechanical stimuli from the microenvironment, like varied substrate stiffness, hydrostatic pressure and active forces on the cell like tension and compression. Recent studies have explored the role of mechanical stimuli on DC aspects of biology like maturation, migration and metabolism. Upon exposure to shear stress using a microfluidic channel, mouse BMDCs show increased surface expression of maturation markers MHC-I and CD86 (Kang *et al.*, 2021). Pressure is another factor that affects DC function. Exposing immature DCs to higher pressure using a Lucite box results in an activation marker profile similar to that of mature cells, and exposing mature DCs to pressure leads to a further increase in the expression of activation markers. Furthermore, increasing pressure on mature DCs also increases the release of inflammatory cytokine IL12 (Craig *et al.*, 2008). Following a similar trend, culturing mouse DCs on stiffer hydrogels leads to increased expression of maturation markers like CD80, CD86 and MHC-II and an increased metabolic profile (Chakraborty *et al.*, 2021). Another study suggests a similar correlation between substrate stiffness and surface markers CD83 and CD86 in human MoDCs; however, the levels of MHC-II remain unchanged (Mennens *et al.*, 2017). Subjecting cyclical strain to mouse DCs also increases the activation of CD40 and MHC-II. However, this increase is not as prominent as mouse DCs matured using lipopolysaccharide (LPS), a bacterial indicator recognised by DC. Cyclical stress also increases the potency of DC to cause T cell proliferation. (Lewis *et al.*, 2013). Taken together, these results suggest that mechanical stress pushes the DCs towards a phenotype closer to that observed during inflammation.

The dependence of mechanical stimuli on DC migration is slightly more complex. Studies have focused on the effects of substrate stiffness on DC motility and migration (Mennens *et al.*, 2017; Bendell *et al.*, 2018; Choi *et al.*, 2021). 2D motility of human DCs (Mennens *et al.*, 2017) and mouse DCs (Bendell *et al.*, 2018) is not dependent on the stiffness of the substrate. In a confined microenvironment, however, the motility of mouse DCs is seen higher on lower

substrate stiffness. Low substrate stiffness is also associated with a more persistent migration (Choi *et al.*, 2021). Furthermore, despite not showing a difference in human MoDC motility, substrate stiffness affects the CCR7 receptor expression, and there is a slight increase in the proportion of transmigrating MoDCs (Mennens *et al.*, 2017). Similarly, exposure to shear stress does not change the migration velocity of mouse DCs but changes the migratory potential of DCs and increases the directionality of the movement (Kang *et al.*, 2021). While these studies provide evidence of the influence of mechanical cues on DC migration, the mechanistic details remain unclear.

Mechanotransduction is the process of sensing and converting external mechanical signals to biochemical signals inside the cells (Martino *et al.*, 2018). Mechanosensitive ion channels are pore forming membrane proteins that get activated upon a mechanical stimulus to the channel or membrane and allow ions to pass through. These ion channels can be selective and may allow only positive ions (Dedman *et al.*, 2009) or negative ions (Qi *et al.*, 2004) to pass through. Mechanosensitive ion channels are the link between mechanical stimuli and biochemical signalling in the cells making them indispensable for mechanotransduction.

Members of the Piezo ion channel family, Piezo1 and Piezo2, are recently discovered mechanosensitive ion channels identified in a mouse neuroblastoma cell line (Coste *et al.*, 2010). Piezo1 and Piezo2 channels are widely expressed in the vertebrate system and are shown to induce mechanically activated currents in many cell types (Coste *et al.*, 2010). Both Piezo1 and Piezo2 are multipass transmembrane ion channels that respond to the force acting on the plasma membrane by getting activated upon increased membrane tension (Lewis and Grandl, 2021). Upon activation, they allow an influx of Ca^{2+} into the cell (Lewis and Grandl, 2021). Ca^{2+} flux is well regulated in immune cells, and Ca^{2+} signalling plays a crucial role in DC migration (Sáez *et al.*, 2018). While the expression of Piezo2 is restricted to the nervous system in humans (Ranade *et al.*, 2014; Woo *et al.*, 2014), Piezo1 is shown to be involved in inflammation and cellular processes in atherosclerosis pathogenesis (Shinge *et al.*, 2022). Furthermore, Piezo1 is also shown to be expressed in a variety of immune cells, such as T cells (Liu *et al.*, 2018; Jairaman *et al.*, 2021) and macrophages (Atcha *et al.*, 2021; Geng *et al.*, 2021). Taken together, the activity and expression profile of Piezo1 makes it a potential candidate for mechanotransduction in immune cells.

Previous studies in the lab have shown the involvement of Piezo1 in T-cell activation and integrin-dependent T cell chemotaxis migration. One study reported the Piezo1 dependence

of downstream signalling upon TCR activation (Liu *et al.*, 2018). The other study focuses on the mechanism of dependence of focal adhesion molecules on Piezo1 during T-cell migration (Liu *et al.*, 2022). The role of Piezo1 on cell migration has been studied in the context of cancer cells, tissue-resident cells like fibroblasts and oligodendrocytes, mesenchymal stem cells and immune cells like macrophages and microglial cells. Piezo1 is shown to induce migration in mesenchymal stem cells and macrophages and cancer development and metastasis (Mousawi *et al.*, 2020; Gao *et al.*, 2021; Wang *et al.*, 2021; He *et al.*, 2022), and shown to inhibit migration in fibroblasts, oligodendrocytes and keratinocytes (Chubinskiy-Nadezhdin *et al.*, 2019; Holt *et al.*, 2021; Velasco-Estevez *et al.*, 2022), depending on the biological context of these cells. These studies highlight Piezo1 as an important player in regulating mechanical cues received by migrating cells.

To the best of our knowledge, the role of Piezo1 in dendritic cell migration has not been studied. Studies have explored the role of Piezo1 in DC metabolism and function in mice. The study by Chakraborty et al. has shown the influence of mechanical stiffness on dendritic cell metabolism and function and implied a role of Piezo1 antitumour response and cytokine release of IL6 and TNFα in mouse DCs (Chakraborty *et al.*, 2021). Another study reports that the deletion of piezo1 in mouse dendritic cells alters the T cell differentiation profile in-vivo (Wang *et al.*, 2022). These studies highlight the importance of Piezo1 in DC biology, providing further motivation to explore the influence of Piezo1 on DC migration.

In this study, we aim to explore the role of Piezo1 in human dendritic cell migration. Using siRNA knockdowns and a piezo1 inhibitor, we have attempted to determine the influence of Piezo1 on the motility and directional migration of human monocyte-derived dendritic cells (MoDCs).

Chapter 2 **Materials and Methods**

2.1 Human Peripheral Blood Mononuclear Cell (PBMC) Isolation and Purification

PBMCs were isolated from leukocyte concentrate (buffy-coat) procured from Tata Medical Center Blood Bank, Kolkata, through approved procedure and clearance from the ethics committee. 4 mL of leukocyte concentrate was diluted with 1x PBS to a total volume of 11 mL. The diluted concentrate was then carefully layered over 4mL of Ficoll (Hisep LSM 1077, Himedia) and then centrifuged for 20 minutes at 25^{o}C at 2500 rpm with a break and acceleration of 1 unit. Upon centrifugation, the buffy coat separates into four layers, with top to bottom being the plasma layer, mononuclear cell layer, Ficoll layer and granulocyte and erythrocyte layer. The plasma layer was discarded, and the mononuclear cell layer was collected in a separate 15 mL falcon. Any remaining Ficoll was washed out by adding 10 mL 1x PBS and palleted down by centrifugation for 5 minutes at 25^{o}C and 1500 rpm.

Any red blood cell (RBC) impurity was removed from the mononuclear cells by RBC lysis in 2 mL of RBC lysis buffer for 5 minutes at room temperature. The lysis reaction was stopped using 3 mL of Magnetic Associated Cell Sorting (MACS) Buffer. The purified mononuclear cells were pelleted down by centrifugation for 5 minutes at 4^{o}C and 1500 rpm.

2.2 CD14+ Human Monocyte Isolation and MoDC generation

Monocytes were isolated from PBMCs using a positive selection of CD14+ cells using a human magnetic activated cell sorting system (MACS). PBMCs were resuspended in 500 µL MACS Buffer, and 8 µL of anti-CD14 magnetic microbeads were added to it. This PBMC-bead solution was incubated while rotating for 20 minutes at 4^{o}C. Any non-specific binding was washed out by adding 3 mL MACS buffer, and the cell pellet was obtained by centrifugation for 5 minutes at 4^{o}C and 1500 rpm. The pallet was then resuspended in 3 mL MACS buffer and the solution was run through a large-size magnetic sorting column after equilibrating the column. After passing the cells, the column was washed with 8 mL MACS and the negative fraction was discarded. The column was separated from the magnet, and CD14+ cells were plunged into a 15 falcon and palleted down by centrifugation.

The cells were then resuspended in RPMI Media. The cell density was adjusted to 0.5 million cells per mL and cells in a total volume of one mL were seeded in a well in 24 well plate. After the monocytes were allowed to culture in the incubator for 30 minutes, 20ng/mL of human recombinant IL4 and 25ng/mL of human recombinant GMCSF was added to the cells. The cells were allowed to culture for 4 days, after which they differentiated into Monocyte-derived Dendritic Cells.

2.3 RNA isolation

RNA was isolated from cells using the TRIzol RNA isolation method. Cells were pelleted down and resuspended in 700 µL of TRIzol, and the solution was transferred to a 1.5 mL tube. For phase separation, 200 µL of chloroform was added to the TRIzol mix, followed by mixing and incubation at RT for 15 minutes in a horizontal position. The samples were then centrifuged at 13500 RPM for 15 minutes at 4ºC. Following centrifugation, the mixture separates into a top aqueous layer, a middle DNA interphase and a lower phenol-chloroform phase. RNA is exclusively present in the top layer, which is carefully collected and added to a new tube containing 0.8 µL of GlycoBlue™ Blue Coprecipitant (Invitrogen), which helps visualise small RNA pellets.

In order to precipitate the RNA, an equal volume of isopropanol was added to the aqueous solution, followed by mixing and incubation at room temperature for 15 minutes. A blue RNA pellet was obtained at the bottom of the tube after centrifugation for 15 minutes at 4ºC and 13500 RPM. The RNA pellet was purified of any residual salts by washing with 750 µL of 75% ethanol and centrifugation for 15 minutes at 4ºC and 13500 RPM. The alcohol was decanted, and the RNA pellet was allowed to dry completely before resuspending in Ambion™ Nuclease Free Water (NFW) for cDNA generation.

2.4 cDNA generation for RT-PCR

cDNA was generated from the isolated RNA using BioRad cDNA preparation kit. 2 µL of RT-Buffer, 2 µL of RT-primer, 2 µL of dNTP and 0.2 µL of reverse transcriptase enzyme was added to a maximum of 1 µg of RNA dissolved in 14 µL of NFW. The reaction mixture was then cycled in the GeneAmp 2400 PCR Thermal cycler (Applied Biosystems) following a standardised protocol.

2.5 Real-Time PCR for gene expression studies

Real-time PCR was carried out in triplicates. We used 18s as a housekeeping gene to calculate the relative expression of a gene of interest using ΔCT values. To each well of a 96 or 384-well RT-PCR plate, 5 µL of SyBr Green, 0.5 µL of _concentration_ forward and reverse primers and 4.5 µL of 1:20 NFW diluted cDNA is added, making the total reaction mixture of 10 µL. Primer-specific gene amplification was performed through multiple cycles of primer dissociation, annealing and elongation in a BioRad RT-PCR cycler with SyBr green detection. The annealing temperature for primers of Piezo1 and Piezo2 was established to be 60ºC. After the amplification cycles, a melt curve determining cycle was added to obtain the melt curves of the PCR products. The melt curves were used to evaluate the specificity of PCR amplification, where a curve with a single peak was the indicator of primer-specific amplification.

2.6 Lipofection of primary human MoDCs

DOTAP liposomal transfection reagent was used to transfect siRNA into human MoDCs. EGFP siRNA was used as a control, and Piezo1-targeted siRNA was used as a target. A solution containing the required siRNA concentration was mixed with an equal volume of a DOTAP solution with 10 times the concentration of siRNA. The mixture was let to incubate at RT for 20 minutes. After the incubation, the DOTAP-siRNA mix was added to cells and cells were allowed to culture in the incubator for the standardised time.

2.7 CFSE staining of cells for live microscopy

Cells were collected, pelleted down and resuspended in 1.5 mL 1X PBS. Cells were stained using cell trace fluorescent CFSE dye by adding 1.5 µL of 1:10 diluted CellTrace CFSE dye to the cell suspension. The cells were incubated at RT in the dark for 10 minutes with intermittent tapping to allow uniform staining. The staining reaction was stopped with 3 mL of RPMI media, and stained cells were pelleted down by centrifugation for 5 minutes at 4ºC and 1500 rpm.

2.8 Live microscopy for 2D cell tracking

Tracking at room temperature

96-well plate were coated with 40 µL of 4 µg/mL recombinant human ICAM1 overnight at 4ºC and washed with 1X PBS. CFSE-stained cells were resuspended in RMPI containing 25

mM HEPES buffer to make the pH CO_2 independent. 30,000 cells in 40 µL volume were seeded on coated wells let to incubate for 45 minutes. Wherever needed, 5 µM GsMTx4 was added while seeding the cells. Cells were allowed to equilibrate at room temperature for 5 minutes before adding CCL19 in the middle of the well. Cells were then allowed to equilibrate on the lens for 5 minutes. A field mainly containing single cells was selected, and images were acquired for 15 minutes every 15 seconds at 40X magnification using the green fluorescent laser in EVOS™ m5000 system.

Tracking at 37°C

Confocal dishes were coated with 200 µL of 10 µg/mL recombinant human fibronectin or 4 µg/mL recombinant human ICAM1 overnight at 4°C and washed with 1X PBS. CFSE-stained cells were resuspended in RMPI containing 25 mM HEPES buffer to make the pH of the media CO_2-independent. 50,000 cells in 200 µL volume were seeded on coated dishes and left to incubate for 45 minutes. Wherever needed, 5 µM GsMTx4 was added while seeding the cells. Post incubation CCL19 was added, and cells were allowed to equilibrate for 10 minutes in the 37°C temperature control set up on the Zeiss LSM confocal system. A time series was recorded for 20 minutes with images taken at an interval of 30 seconds at 10X magnification using a bidirectional 488 nm laser with a speed of 8 and a resolution of 512x512 pixels.

2.9 2D cell tracking analysis

The time series obtained from tracking was opened as a .tiff file in ImageJ. The stack was converted to binary with black background by thresholding using ImageJ. After binarisation, the particles were tracked using a particle tracking plugin in ImageJ called Particle Tracker 2D/3D (Sbalzarini and Koumoutsakos, 2005). The radius parameter was adjusted according to the size of the cells in pixels. The preview of recognised particles was observed, and for the setting where most, if not all, single cells were recognised, the algorithm was allowed to track cells at that setting. As an output, we get the trajectories of all particles, which were saved as a .tiff file. Furthermore, we get the coordinates of each tracked particle at each time point, and the coordinates were saved as a .csv file. A custom-written Jupyter notebook code was used to calculate the path length and MSD for each particle that was tracked for at least 10 minutes at every time point. The MSD for kth frame was calculated using the formula:

$$MSD(k) = \frac{1}{n}\sum_{i=0}^{n} (x_k^i - x_0^i)^2 + (y_k^i - y_0^i)^2$$

$Where\ x_k^i$ is the x coordinate of ith particle at kth frame.

The path length till frame k was calculated as follows:

$$Path\ length\ (k) = \sum_{i=1}^{k} dist(i);$$

$$Where\ dist(i) = \sqrt{(x_i - x_{(i-1)})^2 + (y_i - y_{(i-1)})^2}$$

2.10 Flow cytometry: staining, acquisition and analysis

Flow cytometric was used to check the surface expression of Piezo1 on mature and immature MoDCs. Mature or immature MoDCs were stained for live-lead differentiating violet dye and incubated at 4^{o}C for 30 minutes in 1X PBS. The cells were washed with excess 1X PBS and pelleted down by centrifugation at 4^{o}C, 1500 rpm for 5 minutes. Cells were then surface stained with an antibody cocktail containing anti-TCRβ PE, anti-CD19 PE, anti-CD14 PerCP-Cy5.5, Anti-CD86 FITC and 1: 100 diluted Rabbit anti-human Piezo1 primary antibody for 45 minutes in 1X PBS at 4^{o}C. Post incubation the cells were washed with excess 1X PBS and pelleted down using centrifugation. The cells were then stained with 1:500 diluted goat anti-rabbit Alexa 647 secondary antibody for 30 minutes at 4^{o}C. For control, unstained and secondary control cells (cells stained for surface markers and the secondary antibody without binding for primary Piezo1 antibody) were used. The cells were fixed in 1% PFA after washing with 1X PBS and acquired for flow cytometry.

MoDCs do not have a unique marker to differentiate for positive gating. Instead, we decided to gate CD19- CD14- and TCRβ- cells from live single cells as MoDCs. From the MoDC population, cells expressing with CD86- or CD86^{low} were gated to be immature MoDCs, whereas CD86+ cells were gated to be mature MoDCs. A representative image of the gating strategy for immature and mature MoDCs is shown in Figure M1. The Piezo1 expression levels of mature and immature MoDCs were compared to their respective secondary controls. The geometric mean fluorescence intensity (MFI) was calculated for secondary controls, and Piezo1 stained samples were used as a quantification of the expression of Piezo1.

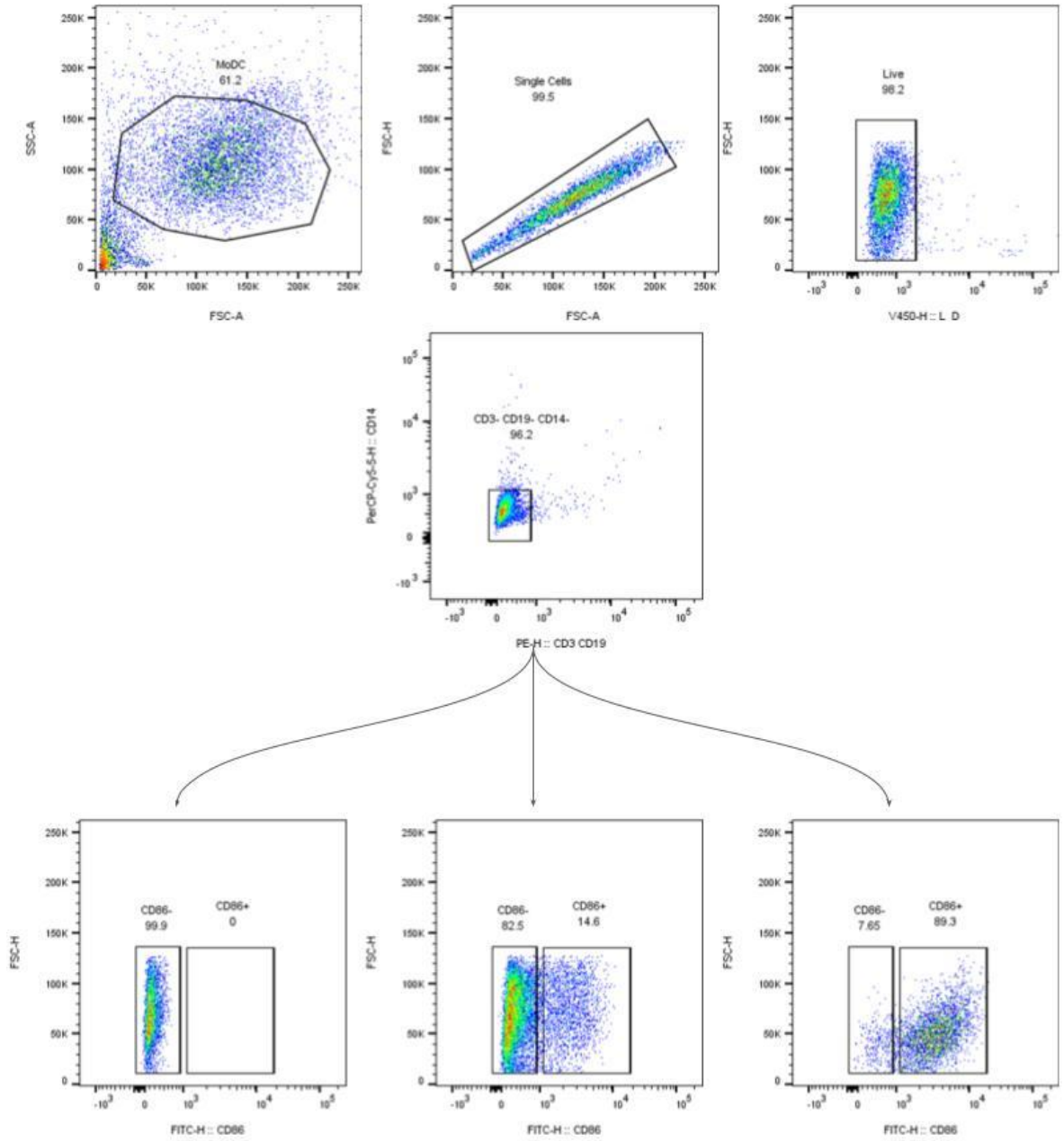

Figure M1 Gating strategy for immature and mature MoDCs

Representative figure of the gating strategy used to gate mature and immature MoDCs. An FSC vs SSC plot separates the cell population from small debris. From the MoDC population, single cells are selected. Live cells are selected from the single cell population. From the live cells CD14- CD19- and CD3- cells are selected as MoDC. From these CD86- cells are selected as immature MoDCs and CD86+ cells as mature MoDCs. The bottom 3 plots represent the representative CD86 expression profiles of unstained (left), immature MoDCs (middle) and mature MoDC (right).

2.11 Fixed immunostaining for confocal Microscopy

Immature MoDCs were seeded on human recombinant fibronectin-coated glass coverslips with a density of about 80,000 cells per coverslip. Seeded cells were incubated in the incubator for 2 hrs, after which 0.5 µg/mL CCL19 was added to the cells where needed and

let to incubate in the incubator for 15 minutes. After the incubation, the coverslips were washed once using filtered 1X PBS, and cells were fixed by incubating for 15 minutes in 4% PFA. The coverslips were then washed 3 times with 1X PBS. Blocking was performed by incubating the cells in a solution of 0.2% triton X-100 in 1X PBS containing 3% bovine serum albumin (BSA) for one hour at room temperature. The coverslips were washed again and incubated overnight at 4^{o}C in a 1:100 dilution of rabbit anti-human piezo1 and mouse anti-human CD44 primary antibody in 1X PBS containing 0.1% BSA. After incubation, the coverslips were washed with 1X PBS and incubated for 45 minutes at room temperature in 1:300 dilution of goat anti-rabbit Alexa-488 conjugated and rat anti-mouse Alexa-633 conjugated secondary antibody in 1X PBS containing 0.1% BSA. After staining, the antibodies were washed again and the stained cells were mounted on Vectashield® mounting media containing DAPI and sealed before confocal imaging. Z stacks of the cells were acquired at 0.5 µm intervals at a magnification of 63x using Zeiss LSM confocal microscope. The images of the cells were generated by maximum intensity z projections of the z stacks using ImageJ.

2.12 Transwell migration assay

Transwell inserts containing pores of size 8 µm were coated overnight with 10 µg/mL human recombinant fibronectin. 0.5 million cells in 50 µL media were added to the transwell without adding media to the lower chamber. For Piezo1 inhibition, 5 µM GsMTx4 was added where needed, and the cells were incubated in the incubator for 45 minutes. After 45 minutes, 500 µL of median containing 0.5 µg/mL CCL19 was added to the lower chamber and the cells were allowed to migrate in response to CCL19 for 3.5 hours in the incubator. After incubation, the migration was stopped by placing the set-up on ice, and the cells in the lower chambers were carefully collected and counted, and the percentage of cells that migrated was calculated.

2.13 µ-migration assay

µ-slide chemotaxis chambers (Ibidi) were coated overnight with 10 µg/mL human recombinant fibronectin. After coating, the chambers were washed with 1X PBS and allowed to dry completely before CFSE-stained cells were seeded in the lower half of the chamber. A final concentration of 0.5 µg/mL was added to the upper chamber, and the set-up was left in the incubator for 45 minutes to allow the cells to settle at the surface and for a stable CCL19

gradient to be established. The chamber was allowed to equilibrate at the lens of the confocal set-up at 37^{o}C for 10 minutes and a time series for 20 minutes at intervals of 30 seconds.

2.14 Statistical analysis

The statistical significance was calculated using GraphPad Prism 8.0. A paired Student t-test was used to calculate the significance of transwell migration data. For other data, an unpaired Student t-test was used.

2.15 Buffer composition

- RBC lysis Buffer (per 500mL volume)
    - 100 µL of 0.5 M EDTA
    - 0.504g of Sodium Bicarbonate
    - 4.145g of Ammonium Chloride
- MACS Buffer
    - 1X PBS
    - 0.5% Bovine Serum Albumin (BSA)
    - 1 mM EDTA

Chapter 3 **Results**

Establishing the experimental set-up to study the role of Piezo1 in DC migration

DCs are a relatively rare population among white blood cells and make up less than 1% of peripheral blood mononuclear cells ((Haller Hasskamp *et al.*, 2005). While it is possible to isolate DCs from peripheral blood, their rare presence in blood makes it a difficult task to use isolated DCs for extensive in vitro studies. It is established that monocytes are DC precursors and, upon inflammation, convert into dendritic cells in vivo (Randolph *et al.*, 1999). It is also established that upon stimulation with cytokines IL4 and GMSCF, monocytes can differentiate into dendritic cells in vitro as well (Chometon *et al.*, 2020). Since monocytes are much more abundant in the peripheral blood, we decided to use monocyte-derived dendritic cells (MoDCs) for in vitro studies. Upon differentiation, these MoDCs are immature and can be converted to mature MoDCs by stimulation with lipopolysaccharide (LPS) (Chometon *et al.*, 2020).

We started by comparing mRNA expression levels of the two piezo proteins, Piezo1 and Piezo2, in mature and immature human MoDCs. RNA was isolated from the cells and converted into cDNA as described in sections 2.3 and 2.4, and the relative expression levels of Piezo1 and Piezo2 were quantified using real-time PCR. The relative expression normalised to Piezo1 in immature MoDCs is plotted in Figure 1B. It was observed that the mRNA expression level of Piezo1 is more than that of Piezo2 in both mature and immature MoDC, with Piezo1 expression being about 10 times higher than that of Piezo2. It was also observed that mature MoDCs show increased Piezo1 and Piezo2 mRNA expression levels compared to immature MoDCs. These results suggest that Piezo1 is the dominantly expressed Piezo family gene in human MoDCs.

With the aim to explore the effect of reduced Piezo1 in MoDCs, we decided to try and knock down Piezo1 in MoDCs. Lipofection has been shown to be an effective method of transient gene knockdown in dendritic cells without causing significant cell death (Martino *et al.*, 2009). We used DOTAP (1,2-dioleoyl-3-trimethylammonium-propane), a cationic lipid transfection reagent, as a carrier as described in section 2.6, to transfect MoDCs with Piezo1 specific siRNA to knockdown Piezo1 expression in the cells. EGFP-specific siRNA was used as a control since EGFP is not expressed in human cells. The incubation time for lipofection

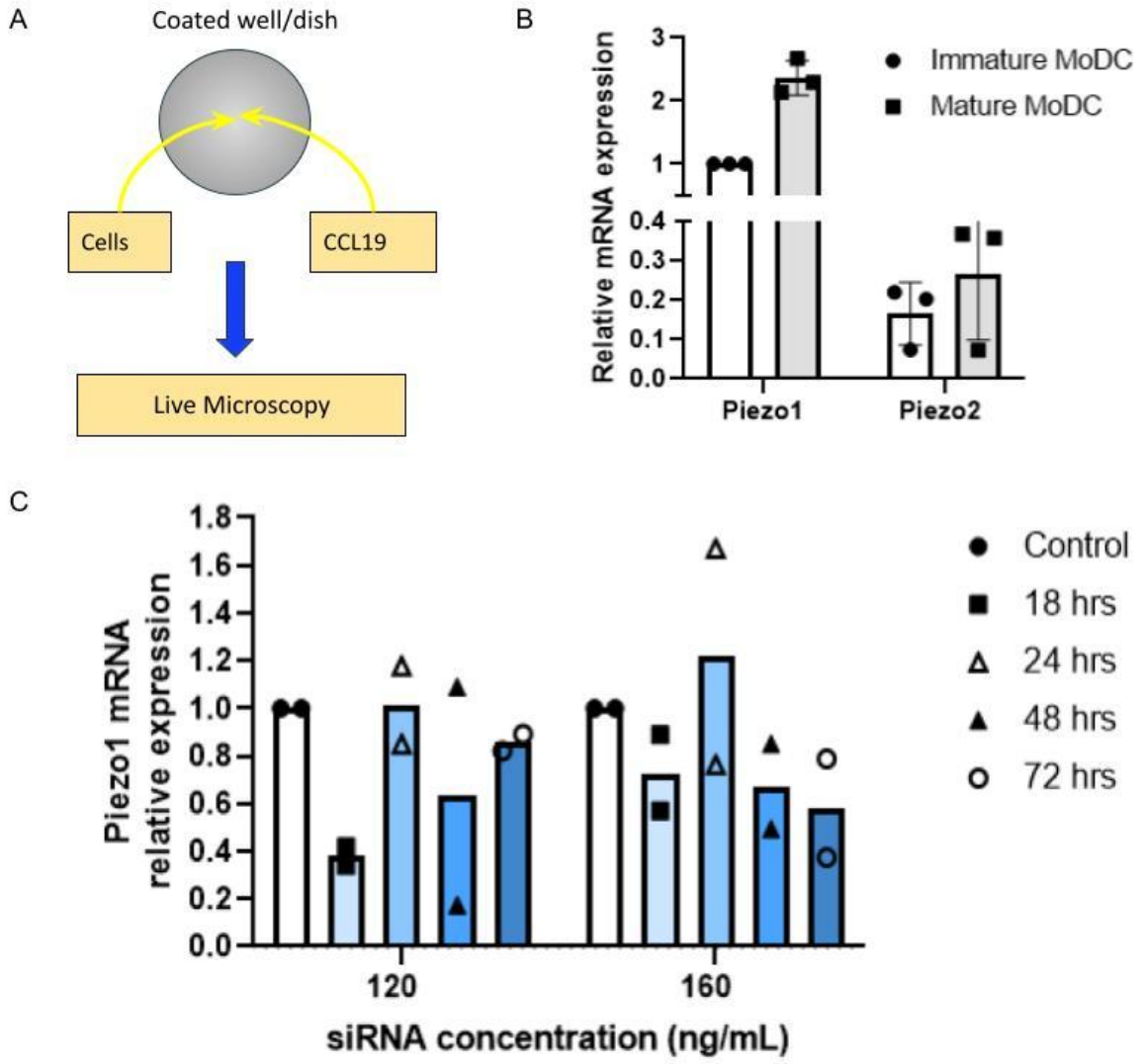

Figure 1 Set up to study the role of Piezo1 in MoDC migration

(A) A schematic diagram of the experimental set-up used to track the motility of MoDCs. **(B)** The mRNA expression of Piezo1 and Piezo2 relative to 18s housekeeping gene on mature and immature MoDCs. The data point represents different donors. The relative mRNA expression is normalised to immature MoDCs Piezo1 expression of respective donors. **(C)** Standardising the dose and incubation for Piezo1 knockdown through lipofection. Relative mRNA expression of Piezo1 at 18, 24, 48 and 72 hours post lipofection, for two doses (120ng/ml and 160 ng/ml) was normalised to the piezo1 expression levels of their respective controls. The data point represents individual values.

was standardised by testing the population mRNA expression levels using RT-PCR at 18,24,48 and 72 hours post lipofection. Gene knockdown response was tested for two doses of siRNA, 120 ng/mL and 160 ng/mL. Figure 1C shows the individual data from different donors and their average values of mRNA expression levels at each time point normalised to their respective controls. A consistent reduction in the mRNA expression levels of greater than or equal to 50% was observed at 18hrs for the dosage 120 ng/mL. Thus we can conclude that transfecting MoDCs with 120 ng/mL of siRNA via DOTAP transfection carrier and incubating for 18 hrs cause a reduction in Piezo1 mRNA levels.

Since DC maturation causes the upregulation of the expression of the chemokine receptor CCR7, they are more responsive to chemokine induced migration. Since Piezo1 mRNA expression levels are also upregulated upon maturation, we decided to focus on the CCL19-induced migration of mature MoDCs. We decided to coat the surface of migration with human intracellular adhesion molecule-1 (ICAM1) as it interacts with a majority of β_2 integrins, which are shown to be involved in DC function and migration (Schittenhelm *et al.*, 2017). As described in sections 2.7 and 2.8, mature MoDCs were seeded, activated by CCL19 and migrated at room temperature. A schematic of the setup used to record and track the migration of cells is shown in Figure 1A.

Effect of Piezo1 knockdown on 2D migration of mature MoDC

Mature MoDCs transfected with control or Piezo1 targeting siRNA were migrated at room temperature, and their mean square displacement (MSD) was compared in the donors where Piezo1 was successfully knocked down. A population mRNA level reduction of 40% or more was considered to be a successful knockdown which was observed in 6 of the 11 donors. The effect of Piezo1 knockdown varied across donors. Figure 2A represents the variation observed across donors, where piezo1 knockdown seems to reduce (Figure 2A left), increase (Figure 2A centre), or not affect (Figure 2A right) the MSD of mature MoDCs. The Piezo1 mRNA levels normalised to respective controls are shown in Figure 2C.

We considered the lack of consistency and a trend in the data and speculated the reason behind it. A reduction in Piezo1 mRNA expression levels does not necessarily translate to a reduction in protein expression, and the protein expression levels at knockdown should be evaluated. Even with a reduced Piezo1 protein expression upon knockdown, the knockdown may not be uniform across all the cells in the culture, giving rise to variability at the single-cell level. While the potential problems so far can be addressed with western blot and flow cytometric analysis, we noticed something peculiar about the migrating cells. Figure 2B shows zoomed representative snapshots of a few migrating cells under the microscope. Note that across the time of 10 minutes, we see the cells changing their position but not their shape. This suggests that the cells may not be actively migrating, and observed movement is due to some external factors.

One potential reason behind this could be a lack of engagement between ICAM1 and dendritic cell surface proteins resulting in improper adhesion between cells and the surface, making it difficult for cells to migrate actively. Less-than-ideal cell health could be another reason behind such observations. The acquisition was not done at physiological conditions,

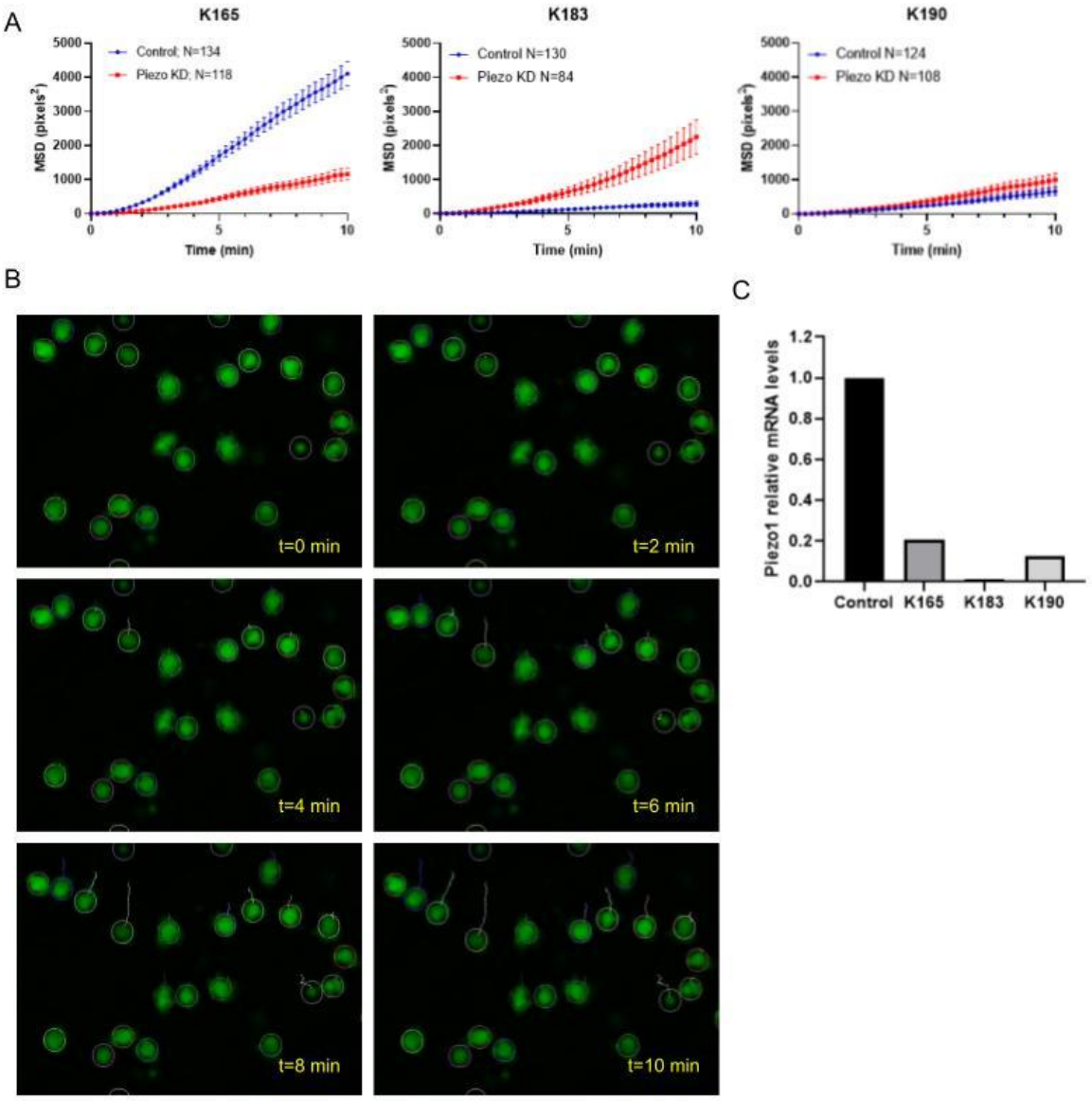

Figure 2 Effects of Piezo1 knockdown on mature MoDC migration

(A) MSD vs time plots for migrating mature MoDCs lipofected with EGFP siRNA (blue) and Piezo1 siRNA (red) for 3 representative donors at room temperature. **(B)** Zoomed snapshots of migrating cells at t = 0,2,4,6,8,10 minutes. The tracked particles are circled and their trajectory is traced as time passes. **(C)** Relative Piezo1 mRNA expression for the same donors as (A). The values are normalized to the Piezo1 expression of the control (EGFP) siRNA-treated cells of the respective donors.

i.e without both 5% CO_2 and regulated 37°C temperature. Furthermore, siRNA transfection is strenuous to cells, and while they looked normal under the microscope, it is a possibility that it may be affecting cell activity and metabolism. Thus, we decided to revise the experimental set up to address the mentioned problems.

The revised experimental set-up to study 2D migration

Since cells weren't actively migrating, we decided to perform the experiment on a confocal microscope which allowed us to track cells at 37°C. The acquisition was done on confocal

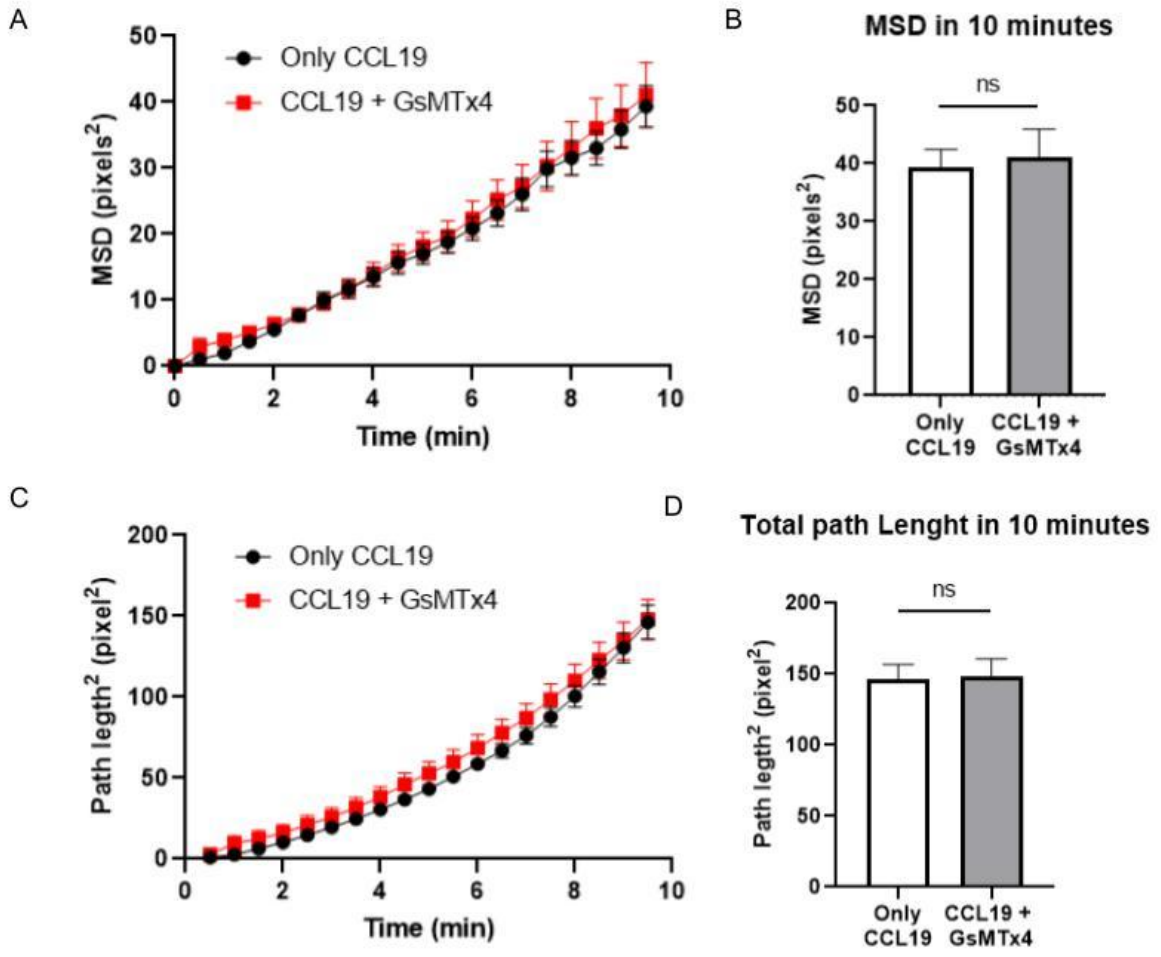

Figure 3 Piezo1 inhibition does not affect mature MoDC motility

MSD **(A)** or Path length^2 **(C)** vs time calculated for mature MoDCs that were allowed to migrate on Retronectin coated confocal dishes after activated by CCL19 only (black) and inhibited by GsMTx4 before CCL19 activation (red). Square of the path length is plotted to help to compare with MSD. MSD **(B)** or Path length^2 **(D)** after 10 minutes of migration compared for statistical significance (for ~300 cells).

dishes instead of wells. Fibronectin is shown to interact with dendritic cells (Jancic *et al.*, 1998)and other studies on DC migration have used fibronectin to coat the surface for migration (Choi *et al.*, 2021); hence instead of ICAM1, we decided to coat the confocal dishes with human recombinant fibronectin (RetroNectin). Due to the limited availability of confocal slots combined with irregularities in siRNA knockdown, we decided to not to use knockdown methods to study the role of Piezo1 until we figured out how to address potential variation at single cell level.

GsMTx4 is a 35 amino acid long peptide, which was isolated from the venom of the spider *Grammostola spatulata* and was shown to block mechanosensitive cationic channels (Suchyna *et al.*, 2000). GsMTx4 is shown to reversibly block the Piezo1 ion channels at µM concentration (C *et al.*, 2011). Since GsMTx4 is a soluble peptide inhibitor, its effect is uniform on cells, and the problem of variation at single cell level is also resolved. Since this

migratory set-up doesn't have any directional CCL19 gradient, we also decided to calculate both the MSD and path length (as elaborated in section 2.9) of the tracked particles.

Piezo1 inhibition does not affect the motility and migration of mature MoDC

As described in section 2.8, we decided to inhibit the Piezo1 ion channel in order to study it's role in 2D mature MoDC migration. Mature MoDCs were migrated over a RetroNectin bed, and tracked at an interval of 30 seconds for 20 minutes at a magnification of 10x at 37^{o}C with and without incubation in GsMTx4 before CCL19 addition. Using this setup, we observed active migration in cells, where moving cells were constantly changing shape. (Video 1) Interestingly, we observed no difference in the MSD and path length of control and GsMTx4-inhibited cells. The results observed were reproducible and Figure 3 represents data from about 300 tracked single cells observed over two donors. Note that in Figure 3C and 3D, the path length^2 is plotted instead of the path length in order to make it directly comparable to MSD. This data suggests that Piezo1 activity is dispensable for 2D migration in mature MoDCs.

Surface Piezo1 gets downregulated upon MoDC maturation

While we were using GsMTx4 to explore the role of Piezo1, we decided to check the surface Piezo1 distribution upon Piezo1 knockdown to try to address the difference in distribution at single cell level upon knockdown. Mature MoDCs were given siRNA treatment as before, and after the incubation time, MoDCs were stained for CD19, TCRβ, CD14 and CD86. To this panel, we added staining for Piezo1 using the primary Piezo1 antibody, followed by staining of the primary antibody using a fluorescent secondary antibody as elaborated in section 2.11. MoDCs stained with surface markers and the secondary antibody without any Piezo1 primary antibody were used as a control (referred to as secondary control), and the fluorescent intensities of the two were compared. Unstained MoDCs were also kept as controls. Upon staining we were unable to see any change in fluorescence from the secondary control (data not shown). We increased the antibody concentration and changed the panel a little and yet we were unable to see any Piezo1-specific staining in CD86+ cells. However, a very tiny fraction of the population was expressing CD86 lower than that observed in mature MoDCs, and it seemed like there was some staining in those cells. This made us question whether the lack of Piezo1 specific staining was not an error in staining but an indication of little to no expression of Piezo1 on mature MoDC surface.

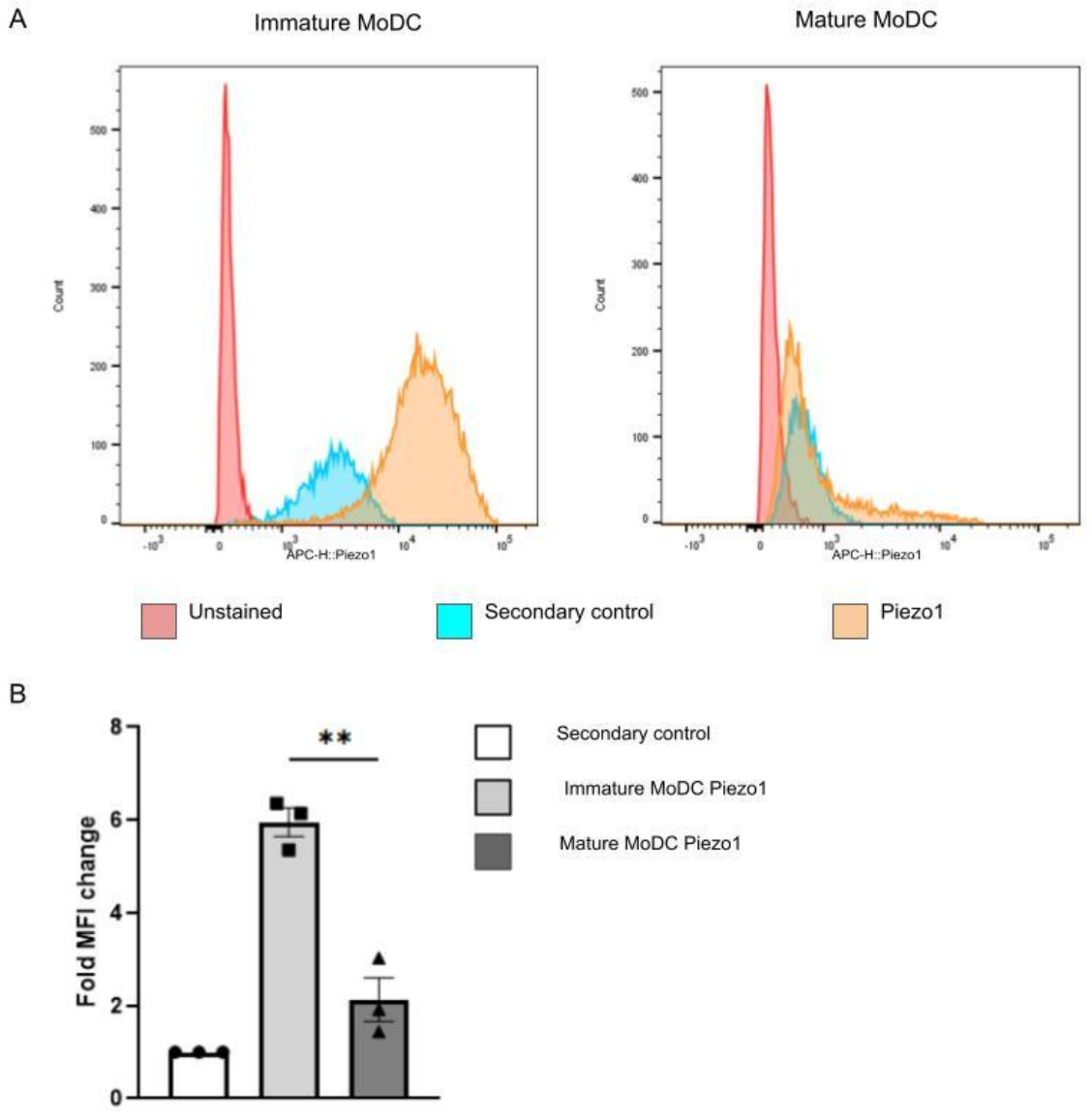

Figure 4 Piezo1 downregulation upon MoDC maturation

(A) Histogram showing the APC specific fluorescence in immature (left) and mature (right) MoDCs, in unstained cells (pink), cells stained with only the goat anti-rabbit Alexa 647 secondary antibody (blue) and cell stained with a rabbit anti-human Piezo1 primary antibody followed by goat anti-rabbit Alexa 647 secondary antibody (orange). **(B)** The geometric mean fluorescent intensity for immature and mature MoDCs as a fraction of their respective secondary controls.

We expected the tiny CD86^{low} population in mature MoDCs to be the immature MoDCs that failed to mature upon LPS stimulation. Hence, we decided to check the surface Piezo1 expression of mature and immature MoDCs since mentioned above using the same panel mentioned above. As expected, we observed a prominent increase in fluorescence from secondary controls in immature MoDCs but little to no increase in mature MoDCs. These observations suggest that as MoDCs maturation and CD86 upregulation, there is a

downregulation in surface Piezo1 expression. These data along with the 2D migration data using GsMTx4 inhibitor suggest that mature MoDCs migrate in a Piezo1-independent manner.

While it is interesting to explore the mechanism and reason behind the downregulation of Piezo1 upon maturation, as well as to evaluate using a controlled experimental set-up whether LPS or maturation-inducing stimuli are, in fact, upstream to Piezo1 expression regulation, it was a difficult task for the time that I had with this project. Instead, we decided to explore the role of Piezo1 in immature MoDC migration.

GsMTx4 inhibition does not change the motility of immature MoDCs in 2D migration

Using the same set-up using RetroNectin-coated confocal dish and live imaging at 37ºC, we compared the MSD and path length^2 in control and Piezo1-inhibited immature MoDCs. When observed the cells were active and moving under the microscope, however, immature cells have a different migratory behaviour to mature cells. In some cases they would migrate in more or less towards a general direction, in other cases they would wander around a little and then move in a general direction as shown in Video 2. It is difficult to ascertain the cause of this behaviour; it may be because sometimes it's taking longer for the cells to equilibrate or this is how their migratory behaviour is.

Since we are interested in the motility of MoDCs, we decided to compare MoDCs when they are undergoing similar migration patterns; specifically, we decided to focus on time frames where they are all moving in a general direction. Interestingly enough, there isn't much of a difference in the distance travelled by the control and GsMTx4 treated cells. The experiment was reproducible and combined data of about 400 cells are shown in Figures 5C and 5D. Comparing the MSD of the control and GsMTx4 treated cells revealed that there is a slight reduction in MSD upon GsMTx4 inhibition, as shown in figures 5A and 5B, however, the difference isn't statistically significant. These results suggest that Piezo1 inhibition does not affect the motility of immature in 2D migration. It also suggests that Piezo1 might affect other aspects of immature MoDC migration.

Piezo1 does not polarise in migrating immature MoDCs

Previous studies in the lab exploring the role of Piezo1 in T-cell migration reported that piezo1 is crucial for effective T cells migration. They further report that upon CCL19

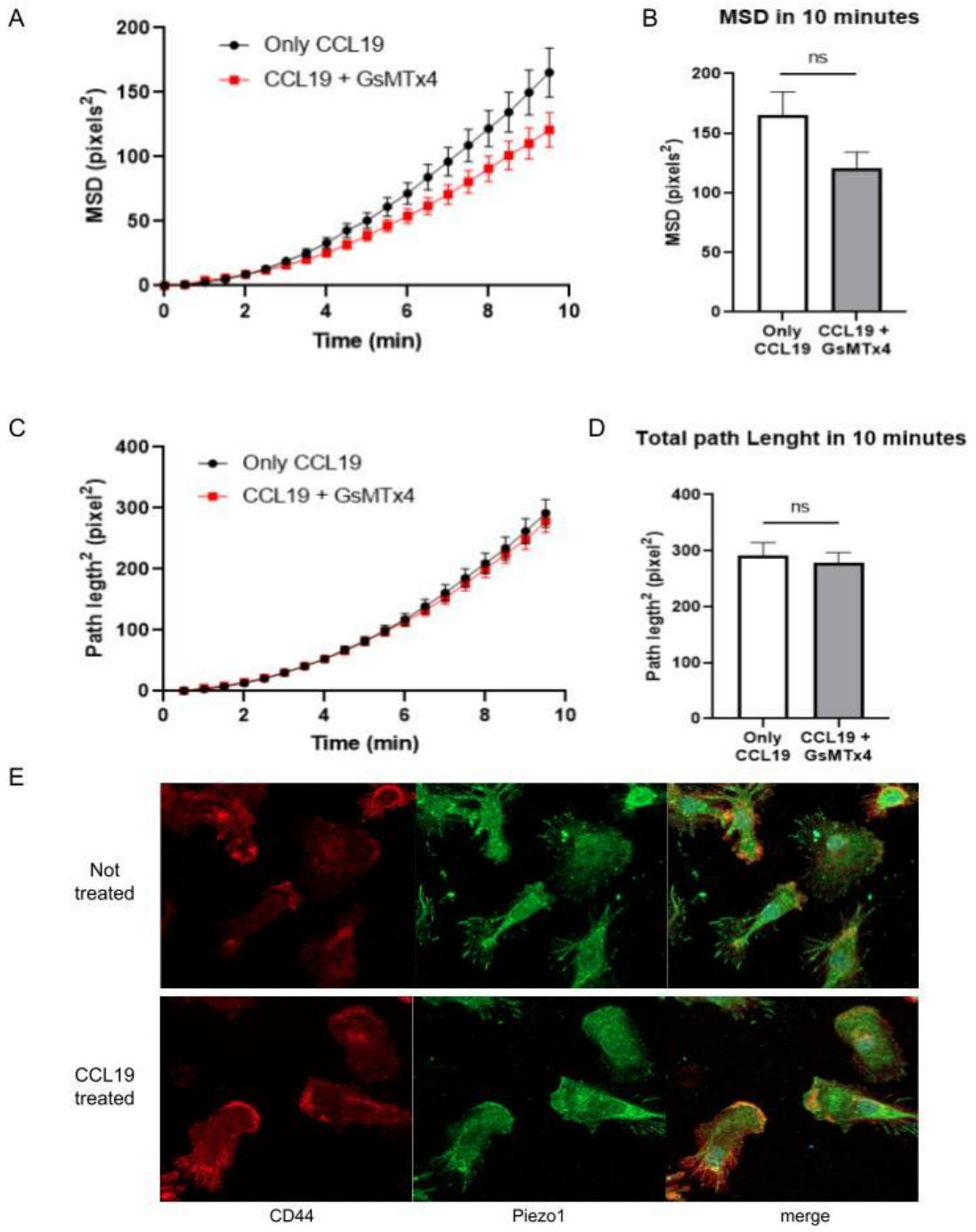

Figure 5 Piezo1 inhibition does not affect mature MoDC motility

MSD **(A)** or Path length **(C)** vs time calculated for mature MoDCs that were allowed to migrate on RetroNectin® coated confocal dishes after activated by CCL19 only (black) and inhibited by GsMTx4 before CCL19 activation (red). Square of the path length is plotted to help to compare with MSD. MSD **(B)** or Path length **(D)** after 10 minutes of migration compared for statistical significance (for ~400 cells). **(E)** Representative images of confocal staining of immature MoDCs with (bottom panel) and without CCL19 activation (top panel). As shown, red represents CD44, green represents Piezo1, blue represents DAPI (individual image not shown) and merged images.

activation, piezo1 polarises in T cells, suggesting a role of piezo1 localisation in migrating T cells (Liu *et al.*, 2022). In contrast to T cells, we couldn't find any significant effect of piezo1 inhibition in 2D migration of immature MoDCs. To further establish the previous

observations, we decided to check if there was any piezo1 polarisation in migrating immature MoDCs. Leukocyte migration involves cytoskeletal polarisation, where they extend a leading edge of actin filaments toward the direction they are migrating in, and microtubules are retraced from the hind part of the cell called the uropod (Vicente-Manzanares and Sánchez-Madrid, 2004). Non-migrating MoDCs and DCs have many projections and could lead to difficulties in differentiating migrating cells from non-migrating ones by their actin distribution under fixed confocal microscopy. Thus in order to observe the polarisation of migrating cells, we decided to stain immunostain CD44, an adhesion molecule shown cluster at the uropod (Vicente-Manzanares and Sánchez-Madrid, 2004) and involved in DC mobilisation (Johnson *et al.*, 2021), along with Piezo1 and DAPI. Cells fixed after the addition of CCL19 were stained and compared to control cells fixed without CCL19 activation and checked for Piezo1 polarisation. As shown in Figure 5E, we see some polarisation expression in CD44, however, we fail to see any polarization in piezo1. These observations further suggest that piezo1 is not involved in the 2D migration of immature MoDCs.

Piezo1 inhibits CCL19-induced 3D transwell migration of immature MoDCs

Since we couldn't find any involvement of Piezo1 in the motility of MoDCs in 2D, we decided to check if it plays any role in 3D chemotactic migration across a membrane using the transwell migration assay. A transwell assay is a migration set up where two plastic hollow chambers are separated by a semi-permeable membrane, as shown in Figure 6A. In the top chamber cells are seeded and chemokine is added in the lower chamber. Cells are attracted towards the chemokine and migrate through the membrane within the time span of a few hours. We used a transwell with a membrane with a pore size of 8 μM and the membrane was coated overnight with RetroNectin to allow cells to adhere and migrate optimally. To explore the role of Piezo1 in 3D chemotaxis migration, an equal number of cells were seeded and incubated in media with (test) and without (control) GsMTx4 for 45 minutes in the top chamber without adding media to the lower chamber. After 45 minutes, chemokine (CCL19) containing media was added to the lower chamber and cells were allowed to migrate for 3.5 hours at the physiological conditions and the migrated cells were counted.

The initial two attempts gave inconsistent results. We realised that while the difference seemed significant, the total number of cells migrated was in the range of 15000-20000 cells. Thus a difference of 5000 cells would look significant, but it could very well have been caused due to counting and sampling errors since we were counting low-density cells,

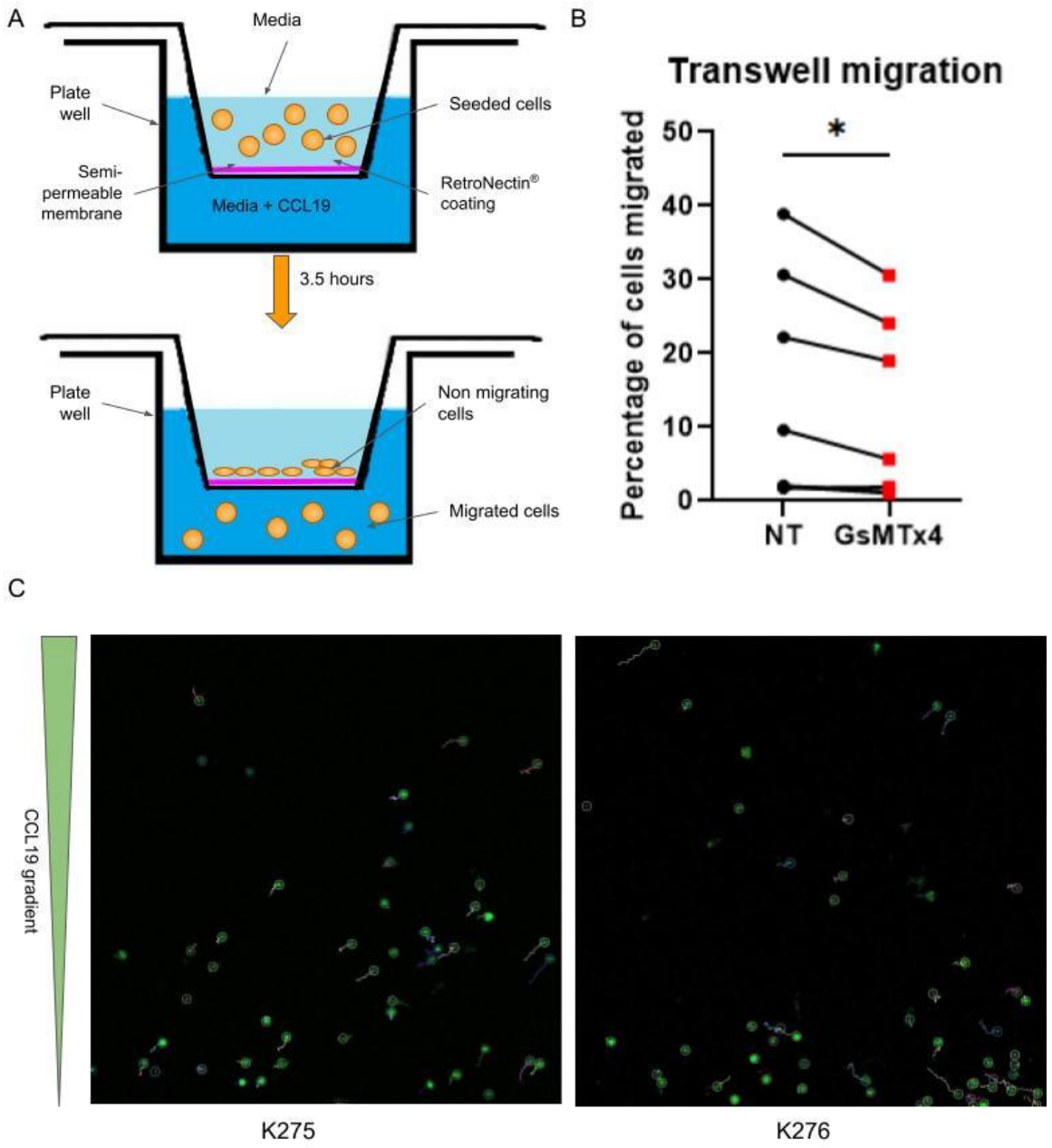

Figure 6 Transmembrane migration and 2D chemotaxis of immature MoDCs

(A) Schematic representation of transwell set up to study the CCL19 induced 3D migration across a membrane. (B) Percentage of cell migrated across the transwell membrane with (red) and without (black) pre-incubation in GsMTx4. (C) Tracked cells and trajectories of immature MoDCs migrating in the chemotaxis chamber. Note the difference in direction of cell migration across the two donors.

resulting in very few cells in each quadrant of the haemocytometer. To account for this, we decided to start with more cells in the top chamber, 0.5 million, as opposed to the 0.2 million cells used before. This experiment was repeated 7 times, out of which, in three donors, there was negligible migration. However, upon checking the cells under the microscope, the cells looked stressed at the end of the experiment, suggesting something unexplained happened to the cells. The remaining four times, we observed that 10-40% of the cells migrated to the lower chamber, with lesser cells migrating than the corresponding controls upon GsMTx4

treatment. The difference was significant when tested using a paired t-test. These data suggest that inhibition of Piezo1 inhibits the transmembrane migration of immature MoDCs.

Effect of Piezo1 inhibition on chemotactic directional migration

The reduction of chemotactic migration in 3D upon Piezo1 inhibition, made us reconsider the implication of slight difference in MSD of immature MoDCs in 2D migration observed upon Piezo1 inhibition. While Piezo1 doesn't seem to affect the motility of immature MoDCs, it is perhaps involved in establishing and maintaining the directionality of migration towards chemotactic cues. We decided to use the Millicell® μ-migration chemotactic assay to further evaluate the role of Piezo1 on the directionality of immature MoDC migration. The Millicell® chamber has microchambers which can establish stable chemokine gradients for hours, making it possible to track and evaluate the migration of cells.

We tried to standardise a protocol for this experimental setup. We decided to stick to the confocal system and acquire the motion of cells at 37^{o}C. Initially, we tried adding the chemokine (CCL19) 10 minutes before the live acquisition of the cells as suggested in the manual. However, we failed to observe any migration in the cells for the 20 minutes of acquisition that followed (images not shown). We wondered if more time was needed for the chemokine to form a stable gradient around the area where the cells are seeded. We decided to add chemokine during the seeding of the cell and let the setup incubate in the incubator for 45 minutes. After incubation, when the migration of cells was recorded we were able to see migration directed towards increased CCL19 concentration as shown in figure 6C left. However, when the experiment was repeated for another donor, we observed that some of the cells were moving towards the CCL19 gradient (top portion of figure 6C right) and some were moving away from the gradient (bottom portion of figure 6C right). This inconsistency in the procedure needs to be addressed if we are to determine the role of Piezo1 inhibition in direction migration accurately.

Chapter 4 Discussion

This study focused on exploring the role of Piezo1 in human MoDCs migration. MoDC migration is influenced by mechanical cues, and Piezo1 is an excellent mechanosensitive candidate for mechanosensation for DC migration. We used CCL19, a migration driving chemokine to induce migration in MoDC and study the migration in vivo. We initially tried using knockdowns to study the role of Piezo1 on MoDC migration at room temperature, however, the cells, with or without Piezo1 knockdown, weren't actively migrating. Multiple factors could have contributed to such behaviour and we decided to use an ion channel specific peptide inhibitor to study the effects of Piezo1 inhibition on mature and immature MoDC motility and directional migration. We observed that the motility of both mature and immature MoDCs in open 2D migration is not affected by Piezo1 inhibition. This observation is thematically in line with previous studies that show no influence of stiffness (Mennens *et al.*, 2017; Bendell *et al.*, 2018) or shear stress (Kang *et al.*, 2021) on human and mouse DC motility. This suggests that the motility or speed of migration in DC is independent of mechanical signals. These observations are also in line with the lack of Piezo1 polarity upon CCL19 activation in 2D in immature MoDCs since previous work in our lab suggests a distinct Piezo1 polarity in CCL19 induced migrating T cells (Liu *et al.*, 2022). Piezo1 inhibition reduces the 3D directional migration of immature MoDCs across a semipermeable membrane. Furthermore, there seems to be a slight reduction in the mean square displacement in immature MoDCs migrating on a 2D field. These results suggest that Piezo1 influences aspects of DC migration other than motility. Results from the Millicell® chemotactic migration would give a broader perspective on the above mentioned observation. Previous studies have reported the influence of substrate stiffness influence DC motility in confined spaces (Choi *et al.*, 2021). Another study has reported changes in directionality upon shear stress on mouse DCs (Kang *et al.*, 2021). The Millicell® chamber is a confined space where we can track the directional migration of cells. If we observe a similar outcome to that of transwell assay, it will allow us to decipher precisely which aspect of MoDC migration is controlled by Piezo1, which will then allow us to form a hypothesis for a downstream mechanism of action. If the outcome of the Millicell® chemotaxis assay is significantly different from that of the transwell assay, it would lead us to explore the physical differences between 3D migration across a membrane and 2D confined migration, such as the volume change required in cells migrating through a membrane (Watkins and Sontheimer, 2011).

Another interesting observation was the downregulation of Piezo1 upon MoDC maturation. This hints towards the possibility that mature MoDCs migrate in a Piezo1-independent manner. We would also need experiments similar to the one shown in this study to establish the independence of Piezo1 in the migration of mature MoDCs. A supposed difference in mechanosensing in mature and immature DCs make thematic sense since many cellular aspects of DCs, like lipid composition and cellular stiffness, are different in immature and mature DCs (Lühr *et al.*, 2020). Furthermore, mature and immature DCs are primarily associated with different ECM profiles (Al-Ashmawy, 2018). Thus exploring the variation of Piezo1 expression across these different profiles would shed more light on the regulatory mechanism of Piezo1 expression.

We also observed that the Piezo1 mRNA expression level in mature MoDCs was greater than that in immature MoDCs. The increase in Piezo1 mRNA is in agreement with a previous study exploring the role of DC piezo1 in T cell differentiation (Wang *et al.*, 2022). While the majority of experiments were performed in DC specific Piezo1 deleted mice, they also performed confirmatory experiments with human MoDCs. Their study suggests that Piezo1 deletion in mice causes the preferred differentiation of T_{reg} over T_H1, and these findings are consistent in experiments done in human MoDCs. They have also demonstrated that stimulation by yoda1, a piezo1 agonist, of LPS-activated human MoDCs increases the release of antitumor cytokines in MoDCs (Wang *et al.*, 2022). This suggests that Piezo1 signalling in dendritic cells works in a pro-inflammatory manner by inducing a T_H1 response in the T cells. As mentioned before, mature MoDCs promote an inflammatory response in the adaptive immune response. Our observation of surface Piezo1 downregulation in matured MoDCs is in contrast with the findings in this paper. Note that while FACS staining, we stained only the surface expression of Piezo1, staining for surface and intracellular Piezo1 will be the first step to understanding the relation of Piezo1 expression with MoDC maturation. Finer mechanistic details about factors regulating the downregulation are required to give more clarity to the contrasting observations between our study and the study by Wang et al.

Thus the study shows preliminary experiments to evaluate the previously unexplored role of Piezo1 in human MoDC migration. These experiments would pave the way for a deeper understanding of the role of Piezo1 in mechanotransduction in DC biology.

List of videos for reference

Video 1 Mature MoDC migration at 37º
Video 2 Immature MoDC migration at 37ºC

References

Al-Ashmawy, GMZ (2018). Dendritic Cell Subsets, Maturation and Function, IntechOpen.

Atcha, H et al. (2021). Mechanically activated ion channel Piezo1 modulates macrophage polarization and stiffness sensing. Nat Commun 12, 3256.

Banchereau, J, and Steinman, RM (1998). Dendritic cells and the control of immunity. Nature 392, 245–252.

Bendell, AC, Anderson, N, Blumenthal, D, Williamson, EK, Chen, CS, Burkhardt, JK, and Hammer, DA (2018). Motile Dendritic Cells Sense and Respond to Substrate Geometry. Ann Biomed Eng 46, 1348–1361.

Bonilla, FA, and Oettgen, HC (2010). Adaptive immunity. J Allergy Clin Immunol 125, S33-40.

C, B, F, S, and Pa, G (2011). The mechanosensitive ion channel Piezo1 is inhibited by the peptide GsMTx4. Biochemistry 50.

Chakraborty, M et al. (2021). Mechanical Stiffness Controls Dendritic Cell Metabolism and Function. Cell Rep 34, 108609.

Choi, Y, Kwon, J-E, and Cho, Y-K (2021). Dendritic Cell Migration Is Tuned by Mechanical Stiffness of the Confining Space. Cells 10.

Chometon, TQ, Siqueira, M da S, Sant´anna, JC, Almeida, MR, Gandini, M, Nogueira, ACM de A, and Antas, PRZ (2020). A protocol for rapid monocyte isolation and generation of singular human monocyte-derived dendritic cells. PLOS ONE 15, e0231132.

Chubinskiy-Nadezhdin, VI, Vasileva, VY, Vassilieva, IO, Sudarikova, AV, Morachevskaya, EA, and Negulyaev, YA (2019). Agonist-induced Piezo1 activation suppresses migration of transformed fibroblasts. Biochem Biophys Res Commun 514, 173–179.

Coste, B, Mathur, J, Schmidt, M, Earley, TJ, Ranade, S, Petrus, MJ, Dubin, AE, and Patapoutian, A (2010). Piezo1 and Piezo2 are essential components of distinct mechanically activated cation channels. Science 330, 55–60.

Craig, DH, Schaubert, KL, Shiratsuchi, H, Kan-Mitchell, J, and Basson, MD (2008). Increased pressure stimulates aberrant dendritic cell maturation. Cell Mol Biol Lett 13, 260.

Dedman, A, Sharif-Naeini, R, Folgering, JHA, Duprat, F, Patel, A, and Honoré, E (2009). The mechano-gated K2P channel TREK-1. Eur Biophys J 38, 293–303.

Förster, R, Davalos-Misslitz, AC, and Rot, A (2008). CCR7 and its ligands: balancing immunity and tolerance. Nat Rev Immunol 8, 362–371.

Gao, L et al. (2021). Suppression of Esophageal Squamous Cell Carcinoma Development by Mechanosensitive Protein Piezo1 Downregulation. ACS Omega 6, 10196–10206.

Geng, J et al. (2021). TLR4 signalling via Piezo1 engages and enhances the macrophage mediated host response during bacterial infection. Nat Commun 12, 3519.

Haller Hasskamp, J, Zapas, JL, and Elias, EG (2005). Dendritic cell counts in the peripheral blood of healthy adults. Am J Hematol 78, 314–315.

He, Y et al. (2022). Myeloid Piezo1 Deletion Protects Renal Fibrosis by Restraining Macrophage Infiltration and Activation. Hypertension 79, 918–931.

Holt, JR, Zeng, W-Z, Evans, EL, Woo, S-H, Ma, S, Abuwarda, H, Loud, M, Patapoutian, A, and Pathak, MM (2021). Spatiotemporal dynamics of PIEZO1 localization controls keratinocyte migration during wound healing. ELife 10, e65415.

Iberg, CA, Jones, A, and Hawiger, D (2017). Dendritic cells as inducers of peripheral tolerance. Trends Immunol 38, 793–804.

Jairaman, A et al. (2021). Piezo1 channels restrain regulatory T cells but are dispensable for effector CD4+ T cell responses. Sci Adv 7, eabg5859.

Jancic, C, Chuluyan, HE, Morelli, A, Larregina, A, Kolkowski, E, Saracco, M, Barboza, M, Leiva, WS, and Fainboim, L (1998). Interactions of dendritic cells with fibronectin and endothelial cells. Immunology 95, 283–290.

Jin, P, Han, TH, Ren, J, Saunders, S, Wang, E, Marincola, FM, and Stroncek, DF (2010). Molecular signatures of maturing dendritic cells: implications for testing the quality of dendritic cell therapies. J Transl Med 8, 4.

Johnson, LA, Banerji, S, Lagerholm, BC, and Jackson, DG (2021). Dendritic cell entry to lymphatic capillaries is orchestrated by CD44 and the hyaluronan glycocalyx. Life Sci Alliance 4, e202000908.

Kang, J-H, Lee, HJ, Kim, O-H, Yun, YJ, Seo, Y-J, and Lee, HJ (2021). Biomechanical forces enhance directed migration and activation of bone marrow-derived dendritic cells. Sci Rep 11, 12106.

Lewis, AH, and Grandl, J (2021). Piezo1 ion channels inherently function as independent mechanotransducers. ELife 10, e70988.

Lewis, JS, Dolgova, N, Chancellor, TJ, Acharya, AP, Karpiak, JV, Lele, TP, and Keselowsky, BG (2013). Dendritic cell activation is influenced by cyclic mechanical strain when cultured on adhesive substrates. Biomaterials 34, 9063.

Liu, CSC et al. (2022). Piezo1 mechanosensing regulates integrin-dependent chemotactic migration in human T cells. 2022.08.16.504114.

Liu, CSC, Raychaudhuri, D, Paul, B, Chakrabarty, Y, Ghosh, AR, Rahaman, O, Talukdar, A, and Ganguly, D (2018). Cutting Edge: Piezo1 Mechanosensors Optimize Human T Cell Activation. J Immunol Baltim Md 1950 200, 1255–1260.

Lühr, JJ et al. (2020). Maturation of Monocyte-Derived DCs Leads to Increased Cellular Stiffness, Higher Membrane Fluidity, and Changed Lipid Composition. Front Immunol 11.

Martino, F, Perestrelo, AR, Vinarský, V, Pagliari, S, and Forte, G (2018). Cellular Mechanotransduction: From Tension to Function. Front Physiol 9.

Martino, S, di Girolamo, I, Tiribuzi, R, D'Angelo, F, Datti, A, and Orlacchio, A (2009). Efficient siRNA Delivery by the Cationic Liposome DOTAP in Human Hematopoietic Stem Cells Differentiating into Dendritic Cells. J Biomed Biotechnol 2009, 410260.

Mennens, SFB, Bolomini-Vittori, M, Weiden, J, Joosten, B, Cambi, A, and van den Dries, K (2017). Substrate stiffness influences phenotype and function of human antigen-presenting dendritic cells. Sci Rep 7, 17511.

Mousawi, F, Peng, H, Li, J, Ponnambalam, S, Roger, S, Zhao, H, Yang, X, and Jiang, L-H (2020). Chemical activation of the Piezo1 channel drives mesenchymal stem cell migration via inducing ATP release and activation of P2 receptor purinergic signaling. Stem Cells 38, 410–421.

Ohl, L, Mohaupt, M, Czeloth, N, Hintzen, G, Kiafard, Z, Zwirner, J, Blankenstein, T, Henning, G, and Förster, R (2004). CCR7 Governs Skin Dendritic Cell Migration under Inflammatory and Steady-State Conditions. Immunity 21, 279–288.

Qi, Z, Kishigami, A, Nakagawa, Y, Iida, H, and Sokabe, M (2004). A Mechanosensitive Anion Channel in Arabidopsis thaliana Mesophyll Cells. Plant Cell Physiol 45, 1704–1708.

Ranade, SS et al. (2014). Piezo2 is the major transducer of mechanical forces for touch sensation in mice. Nature 516, 121–125.

Randolph, GJ, Inaba, K, Robbiani, DF, Steinman, RM, and Muller, WA (1999). Differentiation of phagocytic monocytes into lymph node dendritic cells in vivo. Immunity 11, 753–761.

Sáez, PJ, Sáez, JC, Lennon-Duménil, A-M, and Vargas, P (2018). Role of calcium permeable channels in dendritic cell migration. Curr Opin Immunol 52, 74–80.

Sbalzarini, IF, and Koumoutsakos, P (2005). Feature point tracking and trajectory analysis for video imaging in cell biology. J Struct Biol 151, 182–195.

Schittenhelm, L, Hilkens, CM, and Morrison, VL (2017). β2 Integrins As Regulators of Dendritic Cell, Monocyte, and Macrophage Function. Front Immunol 8.

Shinge, SAU, Zhang, D, Din, AU, Yu, F, and Nie, Y (2022). Emerging Piezo1 signaling in inflammation and atherosclerosis; a potential therapeutic target. Int J Biol Sci 18, 923–941.

Suchyna, TM, Johnson, JH, Hamer, K, Leykam, JF, Gage, DA, Clemo, HF, Baumgarten, CM, and Sachs, F (2000). Identification of a Peptide Toxin from Grammostola spatulata Spider Venom That Blocks Cation-Selective Stretch-Activated Channels. J Gen Physiol 115, 583–598.

Théry, C, and Amigorena, S (2001). The cell biology of antigen presentation in dendritic cells. Curr Opin Immunol 13, 45–51.

Turvey, SE, and Broide, DH (2010). Innate immunity. J Allergy Clin Immunol 125, S24-32.

Velasco-Estevez, M, Koch, N, Klejbor, I, Caratis, F, and Rutkowska, A (2022). Mechanoreceptor Piezo1 Is Downregulated in Multiple Sclerosis Brain and Is Involved in the Maturation and Migration of Oligodendrocytes in vitro. Front Cell Neurosci 16.

Vicente-Manzanares, M, and Sánchez-Madrid, F (2004). Role of the cytoskeleton during leukocyte responses. Nat Rev Immunol 4, 110–122.

Wang, X et al. (2021). Piezo type mechanosensitive ion channel component 1 facilitates gastric cancer omentum metastasis. J Cell Mol Med 25, 2238–2253.

Wang, Y et al. (2022). Dendritic cell Piezo1 directs the differentiation of TH1 and Treg cells in cancer. ELife 11, e79957.

Watkins, S, and Sontheimer, H (2011). Hydrodynamic Cellular Volume Changes Enable Glioma Cell Invasion. J Neurosci 31, 17250–17259.

Woo, S-H et al. (2014). Piezo2 is required for Merkel-cell mechanotransduction. Nature 509, 622–626.

Worbs, T, Hammerschmidt, SI, and Förster, R (2017). Dendritic cell migration in health and disease. Nat Rev Immunol 17, 30–48.